Research Article

Putative Vegetal Inhibitors Against ns2 and vp4 Proteins of African Horse Sickness Virus: Molecular Modelling, Density Functional Theory Analysis, and Toxicokinetic Analysis

Chukwuemeka Calistus Okolo[1]*, Chukwuebuka Valentine Adiole[1], Madubuike Umunna Anyanwu[2], Yewande Tolulope Nejo[3] and Nwakaego Ernestina Nweze[1]

[1]Department of Veterinary Medicine, University of Nigeria Nsukka, 410001 Nsukka, Enugu State Nigeria; [2]Department of Veterinary Microbiology, University of Nigeria Nsukka, 410001 Nsukka, Enugu State Nigeria; [3]Department of Virology, University of Ibadan, Oyo State Nigeria.

Abstract | Outbreak of African horse sickness (AHS) is ongoing in Nigeria. No antiviral is currently licensed for its management, and vaccine failures are rampant. Given Nigeria's rich plant biodiversity, the aim was to use structure-based drug discovery (SBDD) to screen plant-based ligands as potential inhibitors of selected molecular drivers of AHS virus (AHSV) infections. Homology modelling of ns2 and vp4 was done. Binding pockets were predicted on Prank-Web® server. Following preparation of proteins in Biovia-Discovery-Studio®, a collection of 172 ligands were docked separately into ns2 and vp4 proteins of AHSV using PyRx®. Promising ligands were subjected to density functional theory (DFT) analysis in Spartan-14®, and putative toxicokinetic analyses were done in ADMETLAB® 3.0. The ns2 and vp4 proteins of AHSV were successfully double validated using Ramachandran plots and ProSA® tool. The top-40 binding affinity scores (BAS) ranged from -6-8 to -9.3 Kcal/mol, and were recorded from ligands in *Erythrina senegalensis* (9/40), *Cassia occidentalis* (4/40), *Ficus platyphylla* (3/40), *Psidium guajava* (3/40), *Citrullus lanatus* (2/40), *Balanites aegyptiaca* (2/40), *Allium cepa* (2/40) among others. Further, the top 8 hits (alpinumisoflavone, friedelin, epigallocatechin gallate, maniladiol, luteolin, ursolic acid, warangalone, and uzarigenin) had the highest combined (against ns2 and vp4) BAS (-15Kcal/mol to -16.8 Kcal/mol) which were each above that of the reference ligand, aurintricarboxylic acid. Molecular interactions, putative toxicokinetic and DFT analyses predominantly flagged epigallocatechin gallate as a likely potent inhibitor of AHSV. In-vitro evaluation and possible optimization of some of the top-8 hits identified by SBDD against AHSV is warranted.

Editor | Muhammad Abubakar, National Veterinary Laboratories, Park Road, Islamabad, Pakistan.
Received | April 02, 2025; **Accepted** | July 04, 2025; **Published** | August 06, 2025
***Correspondence** | Chukwuemeka Calistus Okolo, Department of Veterinary Medicine, University of Nigeria Nsukka, 410001 Nsukka, Enugu State Nigeria; **Email:** chukwuemeka.okolo@unn.edu.ng
Citation | Okolo, C.C., C.V. Adiole, M.U. Anyanwu, Y.T. Nejo and N.E. Nweze. 2025. Putative vegetal inhibitors against NS2 and VP4 proteins of African horse sickness virus: Molecular modelling, density functional theory analysis, and toxicokinetic analysis. *Veterinary Sciences: Research and Reviews*, 11(2): 146-158.
DOI | https://dx.doi.org/10.17582/journal.vsrr/2025/11.2.146.158
Keywords | African horse sickness virus AHSV, ns2 vp4, Virtual screening, DFT, Epigallocatechin gallate, Plant biodiversity in Nigeria

Introduction

African horse sickness (AHS) remains a critical and often fatal health and welfare challenge of equids in an increasing number of countries. The disease is caused by the African Horse Sickness Virus which belongs to the virus family Reoviridae and is transmitted mainly by hematophagous arthropods of the *Culicoides* genus (Pitchers *et al.*, 2024). Following exposure of susceptible hosts to the virus, it often takes only few days before the onset of viremia characterized by severe symptoms of cardiopulmonary pathologies including fever, petechial hemorrhage, frothy nasal discharge, edema of dependent regions, congestion of the conjunctiva and swelling of the supra-orbital fossa; nearly all up to 90% susceptible horses, consequently die from the disease (Dennis *et al.*, 2019). Although AHSV infections are concentrated in Africa, Middle East and Southwestern Asia, other regions of the globe are currently at risk of AHS outbreak due to climate change drivers of vector migration.

The African horse sickness virus (AHSV) is structurally complex being made of 10 different segments of double stranded RNA encoding seven structural proteins (VP 1-7) and ten non-structural proteins (ns 1, 2, 3, and 3A). The vp4 and ns2 proteins of AHSV were targeted in the current study. The former is a 74 kD minor structural protein which forms a part of the transcription complex of AHSV, and acts as a capping enzyme during AHSV replication, while the latter plays a role in AHSV replication and core assembly by mobilizing viral single stranded RNA to create a replication scaffold (Roy, 2013).

Conventional epidemiological strategies have been used for national and transboundary control of AHSV infection. These strategies include control of international trade, testing and culling of infected animals within AHSV-free zones, and vaccination of susceptible species in endemic zones often by using multivalent live attenuated vaccine (Hopley and Toth 2013; Van Rijn *et al.*, 2020). Some issues have limited the effectiveness of vaccination strategy: one of them are reports (Weyers et al., 2016; Dennis et al., 2019) of genetic re-assortment in preparations of multivalent live attenuated vaccine leading to mutations and acquisition of virulence; moreover, it normally takes a minimum of two (2) weeks before a strong immunity against AHSV is developed in vaccinated hosts. This means that AHS vaccines are of little or no use in active outbreaks. Further, existing anti-AHSV vaccines lack DIVA (differentiating vaccinated from infected) capabilities, thereby further complicating AHS control effort (Dennis *et al.*, 2019). The foregoing highlights the need for investigations focused on identifying or designing potent AHSV antivirals as these will be particularly useful for management of clinical cases of AHS especially in endemic regions or during active outbreaks.

Exploration of plant biodiversity has contributed enormously in development of new chemotherapeutic agents. In fact, it has been estimated that about a quarter of all available drugs are derived from natural products of which plant-derived compounds are a major component (Najmi *et al.*, 2022). Considering the extant threat of disappearance of plant biodiversity, it is also important to document different facets of the medicinal uses of available plants to offer a deeper rationale for their conservation. Further, various herbs have been used in management of viral infection in Nigeria based on anecdotal evidence (Abubakar *et al.*, 2022); it is therefore expected that identification and characterization of the pure antiviral ligands contained in these plants will help in isolating such ligands for enhanced efficacy. Computer aided drug design (CADD) has revolutionized the early stages of drug discovery by leveraging high computing power of modern computers and cloud-based services in identifying potential drug leads that could inform optimization and pre-clinical testing (Singh, 2020; Khusro *et al.*, 2020; Hussain *et al.*, 2022). The objective of this investigation, therefore, was to compare the binding energies, molecular interactions, frontier molecular orbitals, global reactivity descriptors, toxicological and pharmacokinetic parameters of selected ligands found in Nigerian medicinal plants as potential inhibitors of selected drivers of AHSV pathogenesis (vp4 and ns2).

Materials and Methods

Homology modelling, validation, and binding site prediction of ns2 and vp4 proteins of AHSV

The respective amino acid sequences of ns2 protein of AHSV (Entry identification number: A0A189RL52) and vp4 protein (Entry identification number: Q64929) were retrieved from the Uniprot® database (https://www.uniprot.org). Using homologs with over 50% identity and similarities, the vp4 and ns2 sequences were individually subjected to homology

modelling (Waterhouse *et al*., 2018) using the Swiss-Model® platform (https://swissmodel.expassy.org). Built models of ns2 and vp4 were individually validated by analyzing the residue distributions using Ramachandran plot (Laskowski *et al*., 1993; https://saves.mbi.ucla.edu); further validation was done by comparing the Z-scores of the overall model quality of ns2 and vp4 with those of structures generated experimentally, using ProSA tool (Wiederstein and Sippl, 2007). The modelled proteins were uploaded to Prank-Web® server (Jendele, *et al*., 2019; https://prankweb.cz) to generate putative binding sites of the proteins. The best ranked binding pocket for ns2 (probability score: 0.857) and vp4 (probability score: 0.983) were selected for docking of ligand collection.

Ligand selection criteria

The inclusion basis for ligands used in the virtual screening focused on including small molecule present in indigenous herbs anecdotally used for treating viral infection in Nigeria. The plants and their anecdotal use have been reviewed previously (Ukwubile *et al*., 2020; Abubakar *et al*., 2022; Kim *et al*., 2023). Between 2-6 ligands abundant in 40 reviewed plants were selected to create a library of 172 ligands. To serve as reference ligand for comparison, the three dimensional structure of aurintricarboxylic acid (ATA, pubchem ID 2259), a known non-specific in-vitro inhibitor of AHSV (Alonso *et al*., 2020) was included in the ligand array for screening.

Ligand preparation

The 3-D structures of the ligands were downloaded from Pubchem® (https://pubchem.ncbi.nlm.nih.gov) chemical database (Kim *et al*., 2023). The three dimensional structures of the ligands were subjected to energy minimization using the universal force field (UFF) in PyRx® virtual screening software. Thereafter, they were converted to AutoDock Protein Data Bank Partial Charge Atom Type format (*.pdbqt*) using the Open-Babel® module of PyRx®.

Preparation of vp4 and ns2 proteins

Biovia Discovery Studio® Visualizer was used for preparation of modelled ns2 and vp4 proteins of AHSV. The proteins were loaded in Discovery Studio®, and for each of them, water molecules were removed and polar hydrogens were added. Using the AutoDock Vina Wizard® module of PyRx® virtual screening software, *.pdb* versions of ns2 and vp4 were each converted to *.pdbqt* format.

Generation of receptor grid, and molecular docking

The size and coordinates of the best ranked active pockets of ns2 and vp4 were generated in each case by selecting the amino acid residues in the putative pockets using the receptor grid generation tool of PyRx® software (Dallakyan and Olson, 2015). For vp4 protein of AHSV, the center x, y, and z values were 101.914, 27.58523, 153.438 respectively, while the dimensions (Angstrom) values for x, y, and z axes were 32.690, 51.189, and 39.472 respectively. Subsequently, the prepared ligand library was docked into the selected binding site of the vp4 protein. On the other hand, the ns2 proteins receptor grid parameters x, y, z (center) were -14.916, 82.059, and -11.394, respectively, with the dimensions (Angstrom) of x, y, z being 28.977, 40.864, and 40.313, respectively. Likewise, the prepared ligands were docked into the selected binding site of ns2 using the Vina Wizard module integrated in PyRx® with the level of exhaustiveness set at 8 (Dallakyan and Olson, 2015).

Density functional theory analysis

The frontier molecular orbitals and global reactivity descriptors of hit ligands from the screened library were determined and compared using advance theoretical chemistry models. First, a conformer distribution of each ligand was ran; the most stable conformer, subsequently, was used for density functional theory quantum calculations. The B3LYP (Becke, 1993) functional method with 6-31G* basis set (Jensen, 2001) integrated in Spartan 14® computational software was applied, running on HP Pavilion X360, 13th Gen Intel Core i5 - 1335U, @4.4 GHz, 16GB DDR4 ram, and 1TB SSD specification. Quantum mechanical calculations such as highest occupied molecular orbital energy (E_{HOMO}), the lowest unoccupied molecular orbital (E_{LUMO}), band energy gap (Eg), ionization energy (I), chemical hardness (η), electron affinity (A), chemical softness (δ), electronegativity (χ), and dipole moment were computed by applying the following models:

$$Energy\ gap\ (Eg) = E_{LUMO} - E_{HOMO} \quad \ldots.(1)$$

Based on Koopman's theorem (Koopmans, 1934), the ionization energy (I) and the electron affinity (A) can be deduced from the E_{HOMO} and the E_{LUMO}, respectively through Equations 2 and 3 given below:

$$Ionization\ energy\ (I) = -E_{HOMO} \quad \ldots.(2)$$
$$Electron\ affinity\ (A) = -E_{LUMO} \quad \ldots.(3)$$

The electronegativity (χ) and chemical hardness (η) of the ligands were determined based on the Parr and Pearson model (Parr and Pearson, 1983) using Equations 4 and 5 as shown below:

$$\chi = -\mu = (I + A)/2 \quad ....(4)$$
$$\eta = (I - A)/2 \quad ....(5)$$

The chemical softness is given as:

$$\delta = 1/\eta \quad ....(6)$$

Pharmacokinetic/ADMET screening

Putative pharmacokinetic and toxicological parameters –such as molecular properties, intestinal absorption, plasma protein binding ability, enzyme interaction, plasma clearance, heart toxicity, ability to cross blood brain barrier, liver toxicity, acute toxicity, mutagenesis potential and several others of selected hits from the library were predicted by using the Admetlab 3.0® (https://admetlab3.scbdd.com/) server (Fu *et al.*, 2024).

Results

Homology modelling and validation

The ns2 and vp4 proteins of African horse sickness virus were modelled based on experimental ns2 and vp4 proteins of a closely related virus, the bluetongue virus; the new models are presented in Figure 1. These models were validated by subjecting them to Ramachandran plot which revealed that for both the ns2 and vp4 models, over 90% of the amino acid residues are located in the most favored region (Figure 1). Further, when the Z-scores of the overall model quality of ns2 and vp4 were compared with those of structures generated experimentally, the ns2 model had a Z-score of -3.96 falling within the score of structures generated by nuclear magnetic resonance, while vp4 had a Z-score of -7.45 falling within the score of structures generated by x-ray crystallography (Supplementary Figures 1 and 2).

Single and combined binding affinity scores

Table 1 depicts the top forty (40) binding affinity scores (-6-8 to -9.3 Kcal/mol) of ligands against ns2 and vp4 proteins of AHSV in comparison to scores of aurintricarboxylic acid (ATA), which is a known inhibitor of AHSV. Of the top 40 binding ligands from plants found in Nigeria, the following plants contained the following number of hits:

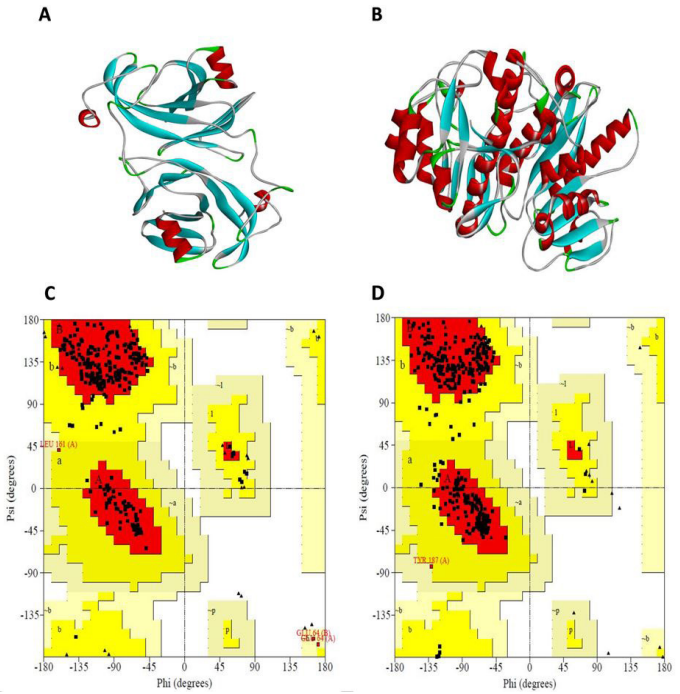

Figure 1: *Modelling and validation of target AHSV proteins. (A) 3-D model of ns2 protein of AHSV based on homology modelling (red = α helices, cyan = β sheets, gray = loops, green = turns). (B) A 3-D Model of vp4 protein of AHSV based on homology modelling (red = α helices, cyan = β sheets, gray = loops, green = turns) (C) Ramachandran plot of modelled ns2 protein of AHSV (plot statistics: residues in most favored regions (A,B,L) = 233 (91.7%); residues in additional allowed regions (a,b,l,p) = 18 (7.1%); residues in generously allowed regions (~a,~b,~l,~p) = 3 (1.2%); residues in disallowed regions = 0 (0.0%); number of non-glycine and non-proline residues = 254 (100.0%); Number of end-residues (excluding Gly and Pro) = 4; number of glycine residues (shown as triangles) = 30; Number of proline residues = 18; total number of residues = 306). (D) Ramachandran plot of modelled vp4 protein of AHSV (plot statistics: residues in most favored regions (A,B,L) = 384 (92.3%); residues in additional allowed regions (a,b,l,p) = 31 (7.5%); residues in generously allowed regions (~a,~b,~l,~p) = 1 (0.2%); residues in disallowed regions = 0 (0.0%); number of non-glycine and non-proline residues = 416 (100.0%); number of end-residues (excluding Gly and Pro) = 2; number of glycine residues (shown as triangles) = 19; number of proline residues = 15; total number of residues = 452).*

Erythrina senegalensis (9/40), *Cassia occidentalis* (4/40), *Ficus platyphylla* (3/40), *Psidium guajava* (3/40), *Citrullus lanatus* (2/40), *Balanites aegyptiaca* (2/40), *Casia tora* (2/40), *Allium cepa* (2/40), *Acacia nilotica* (2/40), while some other plants had only a single ligand in the top 40 binding affinity category. Binding affinity scores of the entire ligand array docked against vp4 protein of AHSV ranged from -3.7 to -9.3 Kcal/mol, and from -2.9 to -8.5 Kcal/mol for those docked against ns2 (Supplementary Table 2); however, the combine docking scores against the two targets (ns2 and vp4) ranged from -7.0 to -16.8 Kcal/mol. Further, Figure 2 shows the top eight hits from the library having the highest combined binding

affinity scores (-15Kcal/mol to -16.8 Kcal/mol) to ns2 and vp4 of AHSV. Alpinumisoflavone had the highest combined binding affinity score (-16.8 Kcal/mol) followed by friedelin, epigallocatechin gallate, maniladiol, ursolic acid, warangalone, and uzarigenin, all of which were above the combine score recorded for the reference ligand, ATA (Figure 2).

Table 1: *Binding affinity (Kcal/mol) of top 40 ligands to ns2 and vp4 proteins of African horse sickness virus.*

S. No	Ligand name	Chemical Formula	PubChem ID	Binding affinity to VP4	Binding affinity to NS2	Typical plants of origin
1.	Warangalone	$C_{25}H_{24}O_5$	5379679	-8.2	-7.9	*Erythrina senegalensis,*
2.	Uzarigenin	$C_{23}H_{34}O_4$	92760	-7.8	-8.2	*Calotropis procera*
3.	Ursolic Acid	$C_{30}H_{48}O_3$	64945	-8.1	-8	*Diospyros mespiliformis*
4.	Triterpenoid	$C_{30}H_{48}O_7S$	451674	-8	-7.8	*Acacia nilotica*
5.	Stigmasterol	$C_{29}H_{48}O$	5280794	-8.3	-7.6	*Cassia tora*
6.	Senegalensin	$C_{25}H_{28}O_5$	124035	-7.4	-7.1	*Erythrina senegalensis*
7.	Quercitrin	$C_{21}H_{20}O_{11}$	5280459	-9.2	-7.5	*Cassia tora; Lannea microcarpa*
8.	Quercetin	$C_{15}H_{10}O_7$	5280343	-8.2	-6.9	*Anogeissus leiocarpus*
9.	Phytosterols	$C_{29}H_{50}O$	12303662	-8.9	-7.1	*Securinega virosa*
10.	Peonidin	$C_{16}H_{13}O_6^+$	441773	-8.3	-7	*Allium cepa*
11.	Pelargonidin	$C_{15}H_{11}O_5^+$	440832	-8.1	-7.1	*Allium cepa*
12.	Myricetin	$C_{15}H_{10}O_8$	5281672	-8.2	-6.9	*Balanites aegyptiaca*
13.	Maniladiol	$C_{30}H_{50}O_2$	397934	-8.1	-8.5	*Erythrina senegalensis*
14.	Mangiferin	$C_{19}H_{18}O_{11}$	5281647	-8.8	-8	*Mangifera indica M*
15.	Luteolin	$C_{15}H_{10}O_6$	5280445	-8.2	-7.9	*Citrullus lanatus*
16.	Lupinifolin	$C_{25}H_{26}O_5$	10250777	-9.1	-7.6	*Erythrina senegalensis*
17.	Lupeol	$C_{30}H_{50}O$	259846	-7.9	-7.4	*Pterocarpus erinaceus*
18.	Lignans	$C_{22}H_{22}O_8$	443013	-6.6	-7.1	*Nicotiana tabacum*
19.	Kaurenoic acid	$C_{20}H_{30}O_2$	73062	-7.9	-7.3	*Annona senegalensis*
20.	Kaempferol	$C_{15}H_{10}O_6$	5280863	-7.8	-7.4	*Balanites aegyptiaca*
21.	Isovitexin	$C_{21}H_{20}O_{10}$	162350	-9	-7.3	*Lannea microcarpa*
22.	Guaijaverin	$C_{20}H_{18}O_{11}$	5481224	-7	-7.2	*Psidium guajava*
23.	Ginsenosides	$C_{30}H_{52}O_2$	3086007	-7.2	-7.1	*Cissus populnea*
24.	Friedelin	$C_{30}H_{50}O$	91472	-8.6	-8	*Pterocarpus erinaceus*
25.	Erythrodiol	$C_{30}H_{50}O_2$	101761	-7.7	-8	*Erythrina senegalensis*
26.	Erybraedin A	$C_{25}H_{28}O_4$	362562	-7.4	-6.9	*Erythrina senegalensis*
27.	Epigallocatechin gallate	$C_{22}H_{18}O_{11}$	65064	-8.9	-7.7	*Psidium guajava*
28.	Epicatechin	$C_{15}H_{14}O_6$	72276	-7.9	-7.5	*Psidium guajava*
29.	Derrone	$C_{20}H_{16}O_5$	14704457	-8	-7.3	*Erythrina senegalensis*
30.	Delphinidin	$C_{15}H_{11}O_7^+$	128853	-7.9	-6.8	*Ficus platyphylla*
31.	Cyanidin	$C_{15}H_{11}O_6^+$	128861	-8.4	-6.8	*Ficus platyphylla*
32.	Chrysophanol	$C_{15}H_{10}O_4$	10208	-7.4	-7.2	*Cassia occidentalis*
33.	Chrysoeriol	$C_{16}H_{12}O_6$	5280666	-7.8	-7.1	*Cassia occidentalis*
34.	Chlorogenic acid	$C_{16}H_{18}O_9$	1794427	-8.1	-6.9	*Citrullus lanatus*
35.	Cianidanol	$C_{15}H_{14}O_6$	9064	-8	-7.7	*Acacia nilotica*
36.	Carpachromene	$C_{20}H_{16}O_5$	10449654	-9.2	-7.5	*Erythrina senegalensis*
37.	Campesterol	$C_{28}H_{48}O$	173183	-9.3	-6.9	*Cassia occidentalis*
38.	Apigenin	$C_{15}H_{10}O_5$	5280443	-7.9	-7.4	*Cassia occidentalis*
39.	Amygdalin	$C_{20}H_{27}NO_{11}$	656516	-8.7	-7	*Ficus platyphylla*
40.	Alpinumisoflavone	$C_{20}H_{16}O_5$	5490139	-8.5	-8.3	*Erythrina senegalensis*
41.	*Aurintricarboxylic acid (ATA)	$C_{22}H_{14}O_9$	2259	-8.2	-7.1	*

**an inorganic broad spectrum antiviral with activity against AHSV used as reference ligand.*

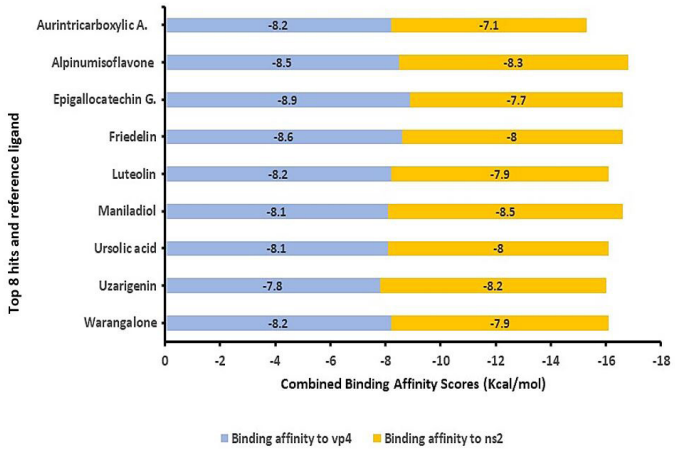

Figure 2: *Combined binding affinity scores of the top eight hits to ns2 and vp4 of AHSV.*

Molecular interactions of ligands at binding pockets of ns2 and vp4

Molecular interactions of the top hits and the reference ligand to the active site of vp4 and ns2 proteins of AHSV are presented in Figure 3 and Supplementary Table 1, respectively. Notably, besides weak Van der Waal forces, maniladiol and friedelin did not make any interaction with amino acid residues at the binding sites of neither ns2 nor vp4 proteins. At the binding pocket of vp4, alpinumisoflavone formed several strong interactions including double pi-cation and double pi-alkyl bonds, single conventional hydrogen, carbon-hydrogen, pi-sigma, pi-pi T-shaped and pi-anion bonds (Figure 3). Likewise, epigallocatechin

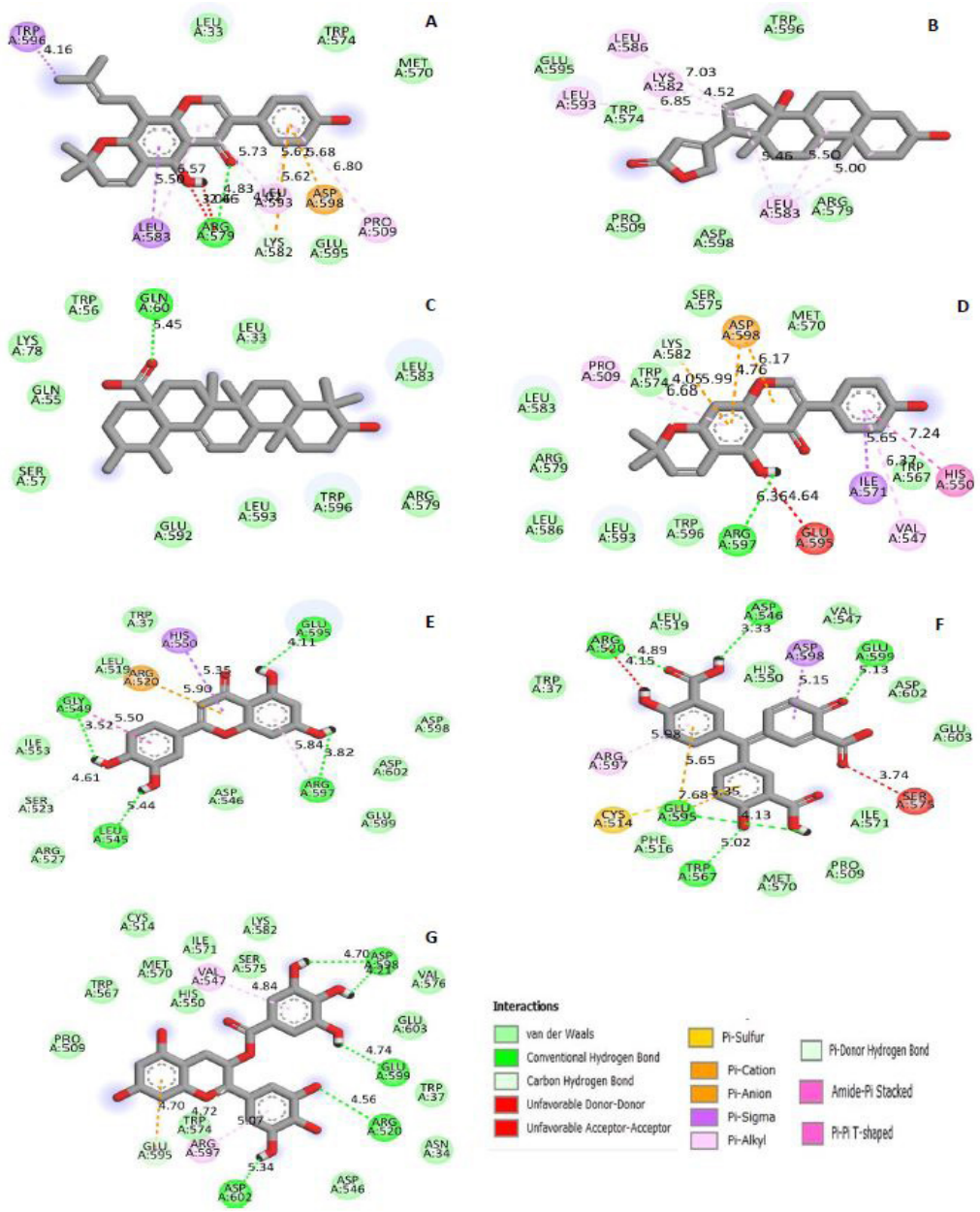

Figure 3: *Molecular interactions of the top binding ligands* to active site of vp4 protein of AHSV.*
*VP4 interaction with: (A) warangalone, (B) uzarigenin, (C) ursolic acid, (D) alpinumisolflavone, (E) luteolin, (F) aurintricarboxylic acid (G) epigallocatechin gallate. *Friedelin and maniladiol made no non-Van der Waal interaction (supplementary fig 3 and 4) and are not shown here.*

Table 2: *Density functional theory analysis (DFT) of the top eight hits and reference ligand targeting ns2 and vp4 proteins of AHSV obtained via DFT at B3LYP/6–31G* level.*

S. No.	Ligands	Molecular weight (AMU)	Electronic energy (AU)	Dipole moment (Debye)	HOMO (Ev)	LUMO (ev)	Eg (eV)	I (eV)	A (eV)	η (eV)	δ (eV^{-1})	μ (eV)	χ (eV)
1.	Warangalone	404.46	-1343.22	1.90	-5.43	-1.40	4.03	5.43	1.40	2.02	0.49	-3.42	3.42
2.	Uzarigenin	374.52	-1197.82	5.60	-6.99	-0.94	6.05	6.99	0.94	3.03	0.33	-3.97	3.97
3.	Ursolic acid	456.71	-1397.77	1.39	-6.05	0.22	6.27	6.05	-0.22	3.14	0.32	-2.92	2.92
4.	Maniladiol	442.73	-1323.73	1.74	-6.07	0.72	6.79	6.07	-0.72	3.39	0.29	-2.68	2.68
5.	Luteolin	286.24	-1028.99	6.43	-5.88	-1.72	4.16	5.88	1.72	2.08	0.48	-3.80	3.80
6.	Friedelin	426.73	-1248.53	3.35	-6.27	-0.24	6.03	6.27	0.24	3.02	0.33	-3.26	3.26
7.	Epigallocatechin gallate	458.38	-1676.61	4.11	-5.55	-1.01	4.54	5.55	1.01	2.27	0.44	-3.28	3.28
8.	Alpinumisoflavone	336.34	-1147.88	1.54	-5.53	-1.46	4.07	5.53	1.46	2.04	0.49	-3.49	3.49
9.	Aurintricarboxylic acid	422.35	-1523.82	6.04	-5.95	-2.85	3.10	5.95	2.85	1.55	0.65	-4.40	4.40

Highest occupied molecular orbital energy (E_{HOMO}), lowest unoccupied molecular orbital energy (E_{LUMO}), energy bandgap (Eg), ionization energy (I), electron affinity (A), chemical hardness, (η), chemical softness (δ), chemical potential (μ), electronegativity (χ).

gallate formed strong four conventional hydrogen bonds, two pi-alkyl bonds, single pi-anion and carbon-hydrogen bonds with amino acid residues at active site of vp4. Warangalone showed over ten interactions with amino acid residues of vp4 binding pocket; however, two of the interactions were unfavourable donor to donor and unfavourable receptor to receptor bonds (Figure 3). Of the twelve interactions formed by the reference ligand, aurintricarboxylic acid, at the vp4 active site, interactions with Arg^{520} and Ser^{575} were unfavorable donor to donor and acceptor to acceptor bonds. At ns2 binding pocket, ursolic acid formed two conventional hydrogen bond with Glu^{94} and Arg^{160}. Beside conventional hydrogen bonds with Phe^{98} and Thr^{102}, and pi-alkyl bond with Ala^{100}, luteolin also formed a strong pi-anion bond with Glu^{99}. Epigallocatechin gallate formed several strong bonds at ns2 binding site including four conventional hydrogen bond, one carbon-hydrogen bond, one pi-donor hydrogen bond, a pi-cation, a pi-sigma and a pi-alkyl bonds. In comparison, the reference ligand also formed several strong bonds at the ns2 active site including four conventional hydrogen bonds, a pi-sulfur bond, a pi-donor bond and a pi-alkyl bond.

Density functional theory analysis of selected hit ligands

The summary of density functional theory analysis (DFT) on ligands of interest is presented in Table 2 to compare the kinetic stability of ligands based on advance chemistry models. Notably, the selected ligands all had molecular weights that fell below 500 AMU. Further, the electronic energies and dipole moment ranged between -1676.61 AU to -1028.99 AU, and between 1.39 to 6.43 Debye respectively. Warangalone, luteolin, epigallocatechin gallate, and alpinumisoflavone had marginally higher E_{HOMO} value when compared to ATA; in contrast, ATA had the lowest E_{LUMO} (-2.85 eV) when compared to all other ligands (Table 2). Likewise, warangalone, luteolin, epigallocatechin gallate, and alpinumisoflavone had lower energy band gap values (4.03 to 4.54 eV) which were comparable with that of the reference ligand. Uzarigenin had the highest ionization energy (6.99 eV); this was followed by friedelin, maniladiol and ursolic acid in that order (Table 2). Conversely, ATA had the highest electron affinity value. Compared with all ligands of interest, the reference ligand ATA had the lowest chemical hardness (1.55 eV) while maniladiol had the highest level of chemical hardness (3.39 eV). Aurintricarboxylic acid had the lowest chemical potential (-4.4 eV) and the highest electronegativity (4.4 eV) whereas maniladiol had the highest chemical potential (-2.68 eV) and the lowest electronegativity (2.68) (Table 2).

Toxicokinetic profiles of selected hit ligands

Table 3 compares the result of the pharmacokinetic analysis of the ligands of interest. All the selected ligands had synthetic accessibility scores (SAS) less than six (6). Only epigallocatechin gallate and ATA acid were predicted to have optimum level of solubility in aqueous solution (LogS between -4 to 0.5 log mol/L). In terms of absorption, friedelin and alpinumisoflavone had the best CaCo-2 permeability values which are greater than -5.15 log cm/s. All the selected ligands had excellent putative human intestinal absorption. Both epigallocatechin and the reference drug were non-inhibitors of P-glycoprotein

Table 3: *Selected toxicokinetic properties of top eight hits and reference ligand docked against ns2 and vp4 of AHSV.*

Parameters	Waran-galone	Uzari-genin	Ursolic acid	Manila diol	Luteo-lin	Friede-lin	Epigallocate chin gallate	Alpinum isoflavone	Aurintricar boxylic acid
SA Score	3.0	4.0	4.0	4	2	4	3	2	2
LogS	-5.097	-4.266	-4.961	-6.028	-4.017	-6.181	-3.483	-4.727	-3.711
Absorption									
Caco2 permeability	-5.031	-5.327	-5.542	-5.354	-5.192	-4.663	-6.894	-4.96	-5.492
HIA	0.006	0.013	0.004	0.001	0.015	0	0.003	0.006	0.002
Pgp inhibitor	0.675	0.034	0.021	0.468	0.001	1.0	0	0.359	0.0
Distribution									
OATP1B3 inhibitor	0.687	0.52	0.893	0.981	0.984	1.0	0.944	0.821	0.983
PPB (%)	95.593	93.594	96.3	97.66	97.642	96.0 84	87.254	97.384	98.895
VDss (L/Kg)	0.139	- 0.226	-0.538	-0.155	-0.614	0.546	-0.293	-0.068	-1.166
BBB (cm/s)	0.129	0.617	0.854	0.991	0.012	0.522	0.003	0.154	0.0
Metabolism									
CYP 1A2 inhibitor	0.0	0.0	0.0	0	1.0	0	0	0.134	1.0
CYP 2C19 inhibitor	1	0.0	0.0	0.301	0.01	0.304	0	0.995	1.0
CYP 2C9 inhibitor	1.0	0.001	0.0	0.836	0.001	0.181	0.206	0.926	1.0
CYP 2D6 inhibitor	0.047	0.0	0.0	0.01	0.578	0.011	0	0.937	0.0
CYP 3A4 inhibitor	0.174	0.0	0.0	0.146	0.998	0.135	0.085	0.819	0.0
Excretion									
CL_{plasma} (ml/min/kg)	4.04	10.504	4.035	12.259	8.482	11.955	8.232	6.01	0.46
$T_{1/2}$ (hr)	1.276	2.124	0.754	0.414	1.373	0.176	2.325	0.875	1.749
Toxicology									
Neurotoxicity	0.529	0.045	0.052	0.074	0.012	0.242	0	0.382	0.071
Nephrotoxicity	0.385	0.909	0.873	0.808	0.01	0.839	0.002	0.276	0.993
hERG blocker	0.104	0.328	0.032	0.049	0.069	0.103	0.049	0.156	0.008
Human hepatotoxicity	0.602	0.744	0.673	0.524	0.367	0.698	0.241	0.516	0.79
Ames mutagenicity	0.622	0.75	0.34	0.337	0.65	0.212	0.845	0.56	0.152
Carcinogenicity	0.73	0.954	0.919	0.932	0.689	0.9	0.272	0.76	0.038
NR Aromatase	0.98	0.705	0.008	0.147	0.727	0.293	0.028	0.979	0.015

SA = synthetic accessibility score, SA score < 6 means easy to synthesize, > 6 means difficult to synthesize. LogS = logarithm of aqueous solubility value, proper solubility value is between -4 to 0.5 log mol/L. Caco-2 = human adenocarcinoma cell line permeability, value > -5.15 log cm/s is normal. HIA = human intestinal absorption, value < 30% shows poor absorption, output value is the probability (0 to 1) of being HIA < 30%. Pgp inhibitor = P-glycoprotein inhibitor, output value is the probability (0 to 1) of being Pgp-inhibitor. OATP1B3 = Organic anion transporting polypeptide 1B3, their inhibition could lead to drug interactions, output value is the probability (0 to 1) of being inhibitor. PPB = plasma protein binding, value < 90% (0.9) means poor PPB which is desirable. VDss = volume of distribution at steady state, values ranging from 0.04-20L/Kg is proper. BBB = blood brain barrier, molecule with logBBB > -1 is BBB+, the output is the probability (0 to 1) of being BBB+. CYP 1A2, CYP 2C19, CYP 2C9, CYP 2D6, CYP 3A4 = are cytochrome P450 isozymes of the liver needed in drug metabolism, the output value for each is the probability (0 to 1) of being an inhibitor of the isozyme. CL_{plasma} = plasma clearance, values >15 ml/min/kg means high clearance, 5-15 ml/min/kg moderate, and <5 ml/min/kg means low clearance. $T_{1\2}$ = half-life, < 1 hour means ultra-short half-life, 1-4 hours means short half-life, 4-8 hours means intermediate half-life, >8 hours means long half-life. Neurotoxicity, nephrotoxicity AMES mutagenesis, human hepatoxicity, carcinogenicity: the output values for each parameter is the probability (0 to 1) of the molecule being toxic. hERG blocker = human ether-a-go-go related gene, hERG blockade could cause cardiac pathologies, the output value is the probability (0 to 1) of being hERG blocker. NR-Aromatase, output value is the probability (0 to 1) of being a endocrine disrupting chemical such as aromatase inhibitor which disturbs androgen-estrogen balance. General empirical decision: 0-0.3: excellent; 0.3-0.7: medium; 0.7-1.0: poor.

while friedelin was an absolute inhibitor (Table 3). In terms of distribution, most of the selected ligand had moderate to high probability (0.5–1.0) of being organic anion transporting polypeptide 1B3 inhibitors. Epigallocatechin gallate had the best (lowest) plasma protein binding while the reference ligand, ATA, gave the worst value (98.89%). Likewise, the reference ligand was predicted to have the worst

volume of distribution (-1.166 L/kg) in comparison to other ligands being considered. The lowest probability of crossing the blood brain barrier was recorded for epigallocatechin and ATA while maniladiol was the most likely to cross the blood brain barrier (probability = 0.99). In terms of metabolism, the reference ligand was a putative inhibitor of all the cytochrome P450 isozymes considered except CYP 2D6 and CYP 3A4, while epigallocatechin gallate, uzarigenin, and ursolic acid were predicted to be non-inhibitors of all the isozymes (Table 3). Plasma clearance time was the first index of drug excretion presented, and the reference ligand was predicted to have the lowest clearance (0.46 mL/min/kg). Epigallocatechin and other ligands had low to moderate level of clearance (<15 mL/min/kg). The half-life of the selected ligands ranged from 0.176 – 2.32 hours, with epigallocatechin having the longest half-life value.

Besides warangalone and alpinumisoflavone which were moderately neurotoxic, all other ligands were non-neurotoxic. The reference ligand, alongside uzarigenin, ursolic acid, maniladiol, and friedelin had high probability of being nephrotoxic (probability = 0.81 to 0.99), while epigallocatechin was not nephrotoxic. All selected ligands were not human-ether-a-go-go related gene blockers except uzarigenin which showed a low to moderate probability (0.328) of being a blocker. Apart from epigallocatechin gallate, all the selected ligands had moderate to high probabilities of being hepatotoxic. The reference ligand had the least probability (0.152) of being AMES mutagenic while epigallocatechin had the highest probability (0.845); however, epigallocatechin had a very low probability of being carcinogenic (0.27) at the same time. Finally, epigallocatechin gallate, aurintricarboxyic acid, ursolic acid, maniladiol, and friedelin all had low probabilities (< 0.3) of being an endocrine disrupting chemical or NR aromatase inhibitor.

Discussion

Two drivers of replication and pathogenesis of African horse sickness virus (AHSV) (ns2 and vp4) were targeted in this study. It is conceivable that the inhibitory potential of a ligand against a pathogen would directly correlate with the size of the combined negative binding affinity scores of the ligand to relevant targets of the pathogen. Several reports have employed this strategy in vaccine design and in computer aided drug design (Raj and Varadwaj, 2016). The ns2 and vp4 models of AHSV built in this current study gave high validation scores. Analysis of the Ramachandran plot showed both ns2 and vp4 models had more than 90% of their amino acid residues in the most favorable region with 0% of the residues lying in the disallowed region of the plot in both cases.

A list of Nigerian plants having more than one strongly binding ligands to ns2 or vp4 of AHSV was provided; it however must be interpreted in the context of the top 40 hits (Table 1) flagged by virtual screening of the library of ligands selected for this study. Their comparatively higher binding scores highlights their potential as anti-AHSV chemicals, barring other limitations. Another potential implication is that various combinations of the listed plants may be good candidates for ayurvedic or herbal medical preparations against AHSV provided good consideration has been made for toxicity and posology. The growing attention on therapeutic potential of plant based medicine has been noted in various reports (Ukwubile *et al.*, 2020; Abubakar *et al.*, 2022), especially in developing countries where advance pharmaceutical and medical technologies may be limited. Remarkably, the reference drug, ATA, came behind the top 8 hits in terms of combined binding affinity scores, implying that the top 8 hits are likely to bind to the AHSV targets with comparatively more avidity than ATA. The inhibitory activity of ATA on AHSV replication has been demonstrated *in vitro*, however, the exact mechanism of action of the ligand is not clearly known hence it is considered a non-specific inhibitor (Alonso *et al.*, 2020). It is also possible that ATA may be acting by mechanisms different from interaction with vp4 and ns2 proteins of AHSV.

Among the top 8 hits, friedelin and maniladiol are the least likely to make good drug candidates because they formed no strong molecular interaction at the active sites of ns2 and vp4, their high binding scores notwithstanding. Both ligands predominantly formed Van der Waal interactions at the sites. Van der Waal forces are electrostatic forces that are weak in nature, spanning only short distances and commonly seen within neutral molecules (Parsegian, 2005). In contrast some other ligands such as epigallocatechin and warangalone showed a better likelihood of being antiviral hits by establishing several strong covalent and conventional hydrogen bond with amino acid residues at ns2 and vp4 active sites. It is instructive to note that although the reference drug ATA formed

strong hydrogen and covalent bonds with vp4, it also formed unfavourable donor to donor and acceptor to acceptor bonds with Arg^{520} and Ser^{575}. Ionic, covalent, hydrogen, and Van der Waal bonds are all cohesive bonds in their descending order of strength (Jeffrey and Saenger, 2012), however, unfavourable donor to donor or acceptor to acceptor bonds are not desirable since it may produce repulsion.

A list of potential antiviral hits could be further screened based on their reactivity, stability and physicochemical properties as computed by advance chemistry and quantum mechanical models. Luteolin and ATA had the highest dipole momentum -a property that indicates their high hydrophilicity relative to other ligands. When drug candidates are strongly hydrophilic, there are less likely to be able to penetrate cellular lipid bilayer of cells in sufficiently therapeutic dose to act. It is conceivable that this could be one of the reasons ATA is reported to be ineffective *in-vivo* notwithstanding its *in-vitro* effectiveness against AHSV (Alonso *et al*., 2020). While E_{HOMO} of a ligand describes its molecular orbital that is electron-rich and that can easily donate electron, the E_{LUMO} describes its orbital which easily accepts electron. Data from the current study showed that warangalone, alpinumisoflavone, and epigallocatechin gallate had highest E_{HOMO} while ATA, luteolin and alpinumisoflavone had the lowest $E_{LUMO.}$ Often it is desirable that a drug candidate is sufficiently reactive rather than inert; a combination of a high E_{HOMO} and low E_{LUMO} values are therefore preferred (Ishabiyi *et al*., 2023). A perhaps more critical parameter for evaluating potential reactivity and bioactivity of lead ligands is the band energy gap (Ev) which factors in both the E_{HOMO} and E_{LUMO}. In frontier molecular orbital theory, it is thought that wide energy gap value increases stability and adversely affects the movement of electrons leading to poor affinity between the ligands and the binding pockets of their target (Balogun *et al*., 2022; Ishabiyi *et al*., 2023), hence ATA, warangalone, alpinumisoflavone, luteolin and epigallocatechin gallate, having relatively smaller energy band gaps, are potentially the most reactive ligands.

The top 8 hits and ATA could all be easily synthesized given that their predicted synthetic accessibility (SA) scores were all below 6; it will however be one level easier to synthesize ATA or alpinumisoflavone (SA=2) than to synthesize epigallocatechin (SA = 3). Absorption of the ligands were compared by prediction of the human colon adenocarcinoma cell line permeability (caco2), P-glycoprotein inhibition, and human intestinal absorption (HIA) values. Caco2 is structurally and functionally similar to the intestinal epithelium, hence in-vivo permeability of substances through it, is a good estimate of oral absorption; further, HIA levels less than 30% is considered poor (Fu *et al*., 2024). The top 8 hits and ATA appear to be well absorbed intestinally. The p-glycoprotein (MDR1) is an efflux transporter found on cell membrane of intestinal epithelial cells and some other tissues; substances that inhibit it are likely to be well orally absorbed, and these include friedelin, warangalone, maniladiol, and alpinumisoflavone to lesser extent. Comparing the indices of distribution, it is obvious that they all have a high probability of inhibiting OATP1B3 – a crucial hepatic uptake transporter (Keppler, 2014), inhibition of which predisposes the patient to drug interaction- hence all the ligand are likely to take part in drug interactions. Among the selected ligands, only epigallocatechin has a plasma protein binding value that is below 90%; this implies that this agent will be more biologically available to body cells. When drugs are highly bound to plasma protein, free drug concentration in the serum may be reduced below therapeutic levels. Further, when entry across the blood brain barrier (BBB) was considered, epigallocatechin and ATA were the least likely to cross the BBB. This is a desirable feature for drugs with peripheral target or potential CNS side effects, but an undesirable one if its targets are in the CNS. The cytochrome P450 isozymes play critical roles in phase I and II reactions of drug metabolism (Coleman, 2020; Hedaya, 2023). By having the least probability of inhibiting any of the cytochrome P450 isozymes considered, epigallocatechin gallate, ursolic acid and uzarigenin are likely to be easily metabolized and eliminated, causing minimal drug interactions in the body, unlike ATA which inhibited most of the cytochrome P450 isoenzymes. Plasma clearance is a critical pharmacokinetic property because it is important in dose determination, and describes the overall drug exposure in the system at a steady state (Hedaya, 2023). ATA will be quickly eliminated from plasma since it has a very high clearance (0.46 ml/min/kg) unlike epigallocatechin gallate which has a medium plasma clearance level. Likewise, epigallocatechin gallate may have a delayed onset of action but its effects are likely to persist for a longer period because data from this study suggest that it

has a markedly longer half-life when compared to the other ligands.

Putative toxicity data presented in this study suggest that epigallocatechin gallate is relatively less toxic when compared to the other top hits and the reference ligand. Epigallocatechin gallate was predicted to be non-neurotoxic, non-nephrotoxic, non-hepatotoxic, non-cardiotoxic (non-blocker of hERG), and a non-endocrine-dirsrupting-chemical (non-inhibitor of NR aromatase). Although a high probability of being AMES mutagenic was predicted for epigallocatechin gallate, it has been shown that mutagenicity does not always imply to carcinogenicity (Barnes *et al*., 2018). In fact, the data from this study classified epigallocatechin gallate as being non-carcinogenic at the same time it was predicted to be AMES mutagenic. In contrast, ATA and the other ligands were flagged as being toxic in at least three or more systems. The ramification of the foregoing is that if laboratory data proves that epigallocatechin gallate is indeed AMES mutagenic, there is an absolute need for its optimization by chemical modification for improved safety profile in patients; and if all else fails in terms of safety, this compound in its pure form could potentially be an extremely useful anti-AHSV laboratory agent for research, or a potent anti-AHSV disinfectant.

The limitation of this study is that free binding energies of the ligand library to the viral targets could not be determined due to computational limitations: for most of the hits, the force-fields generated for molecular dynamics simulation (MDS) in GROMACS had penalty scores that are several times (5-10 times) higher than 10, hence, the MDS trajectory and free binding energy of the ligands could not be accurately determined, and experimental validation is highly recommended (Abraham *et al*., 2024)-a path that is outside the scope of the current study. However, to the best of our knowledge, the findings from this work is the first attempt at identifying and describing the molecular interactions, physicochemical and toxicokinetic characteristics of pure anti-AHSV ligands founds in Nigerian plants anecdotally used against viral infection. At a moment where repeated outbreaks of AHSV is rampant in Nigeria, data from this work provides insight for further investigation including experimental binding affinity (K_D) determination and preclinical efficacy studies.

Conclusion

In conclusion, ns2 and vp4 proteins of AHSV were modelled, and targeted by a collection of potential inhibitors of plant origin using structure based drug design approach. The top 8 hits were alpinumisoflavone friedelin, epigallocatechin gallate, maniladiol, ursolic acid, warangalone, and uzarigenin which had higher combined (against ns2 and vp4) binding affinity scores (-15Kcal/mol to -16.8 Kcal/mol) than the reference ligand ATA. Density functional theory and toxicokinetic evaluations predominantly flagged epigallocatechin gallate as a likely potent inhibitor of AHSV. *In-vitro* testing against AHSV, and possible hit optimization of any of the selected compounds is warranted.

Acknowledgements

This work is supported by the small grant series of TETFund Nigeria (TETFund IBR reference number: TETF/DR&D/CE/UNI/NSUKKA/BR/2024/VOL.1

Novelty Statement

This study provides in-silico evidence to support the inhibition of selected molecular drivers of African horse sickness infection by epigallocatechin gallate which is found in identified tropical plants.

Author's Contribution

Chukwuemeka C. Okolo: Conceptualization, funding, methodology, software, data curation, original draft preparation.
Chukwuebuka V. Adiole: Methodology, data curation.
Madubuike U. Anyanwu: Conceptualization, data curation, reviewing and editing.
Yewande T. Nejo: Conceptualization, data curation, reviewing and editing.
Nwakaego E. Nweze: Conceptualization, funding, data curation, reviewing and editing.

Funding
This work is supported by the small grant series of TET Fund Nigeria (TET Fund IBR reference number: TETF/DR&D/CE/UNI/NSUKKA/BR/2024/VOL.1

Data availability

All the data that are relevant to the study are included in the article and uploaded as supplementary information.

Ethical approval

Not applicable

Consent to participate

Not applicable

Supplementary material

There is supplementary material associated with this article. Access the material online at:

Conflict of interest

The authors have declared no conflict of interest.

References

Abraham, M., Alekseenko, A., Basov, V., Bergh, C., Briand, E., Brown, A., Doijade, M., Fiorin, G., Fleischmann, S., Gorelov, S., Gouaillardet, G., Grey, A., Irrgang, M.E., Jalalypour, F., Jordan, J., Kutzner, C., Lemkul, J. A., Lundborg, M., Merz, P. and Lindahl, E., 2024. GROMACS 2024.1 Manual (2024.1). Zenodo.

Abubakar, I.B., Kankara, S.S., Malami, I., Danjuma, J.B., Muhammad, Y.Z., Yahaya, H. and Nurudeen Q.O., 2022. Traditional medicinal plants used for treating emerging and re-emerging viral diseases in northern Nigeria. Eur. J. Integr. Med., 49(102094): 102094. https://doi.org/10.1016/j.eujim.2021.102094

Alonso, C,, Utrilla-Trigo, S,, Calvo-Pinilla, E,, Jiménez-Cabello, L,, Ortego, J. and Nogales, A., 2020. Inhibition of Orbivirus replication by aurintricarboxylic acid. Int. J. Mol. Sci., 21(19): 7294. https://doi.org/10.3390/ijms21197294

Balogun, T.A, Chukwudozie, O.S., Ogbodo, U.C., Junaid, I.O., Sunday, O.A., Ige O.M. and Sabatier, J.M., 2022. Discovery of putative inhibitors against main drivers of SARS-CoV-2 infection: Insight from quantum mechanical evaluation and molecular modeling. Front. Chem., 10: 964446. https://doi.org/10.3389/fchem.2022.964446

Barnes, J.L., Zubair, M., John, K., Poirier, M.C. and Martin, F.L., 2018. Carcinogens and DNA damage. Biochem. Soc. Trans., 46(5): 1213-1224. https://doi.org/10.1042/BST20180519

Becke, A.D., 1993. Density-functional thermochemistry. III. The role of exact exchange. J. Chem. Phys, 98: 5648-5652. https://doi.org/10.1063/1.464913

Coleman, M.D., 2020. Human drug metabolism. John Wiley and Sons. https://doi.org/10.1002/9781119658016

Dallakyan, S. and Olson, A.J., 2015. Small-molecule library screening by docking with PyRx. Methods Mol. Biol., 1263: 243-250. https://doi.org/10.1007/978-1-4939-2269-7_19

Dennis, S.J., Meyers, A.E, Hitzeroth, I.I. and Rybicki, E.P., 2019. African horse sickness: A review of current understanding and vaccine development. Viruses, 11(9): 844. https://doi.org/10.3390/v11090844

Fu, L., Shi, S., Yi, J., Wang, N., He, Y., Wu, Z. and Cao, D., 2024. ADMETlab 3.0: An updated comprehensive online ADMET prediction platform enhanced with broader coverage, improved performance, API functionality and decision support. Nucl. Acids Res., 52(W1): W422-W431. https://doi.org/10.1093/nar/gkae236

Hedaya, M.A., 2023. Basic Pharmacokinetics. Routledge. https://doi.org/10.4324/9781003161523

Hopley, R. and Toth, B., 2013. Focus on African horse sickness. Vet. Rec., 173(1): 13-14. https://doi.org/10.1136/vr.f4250

Hussain, A., Jairajpuri, D.S., Anwar, S., Choudhury, A., Hawwal, M.F., Firdous, A., Alajmi, M.F. and Hassan M.I., 2025. Apigenin-mediated MARK4 inhibition: A novel approach in advancing Alzheimer's disease therapeutics. Mol. Diversity, 22: 1-2. https://doi.org/10.1007/s11030-025-11104-x

Ishabiyi, F.O., Ogidi, J.O., Olukade, B.A., Amorha, C.C., El-Sharkawy, L.Y., Okolo, C.C., Adeniyi, T.M., Atasie, N.H., Ibrahim, A. and Balogun, T.A. 2023. Computational evaluation of Azadirachta indica-derived bioactive compounds as potential inhibitors of NLRP3 in the treatment of Alzheimer's disease. J. Alzheimers Dis., 94(s1): S67-S85. https://doi.org/10.3233/JAD-221020

Jeffrey, G.A. and Saenger, W., 2012. Hydrogen bonding in biological structures. Springer Science and Business Media.

Jendele, L., Krivak, R., Skoda, P., Novotny, M. and Hoksza, D., 2019. PrankWeb: A web server for

ligand binding site prediction and visualization. Nucl. Acids Res., 47(W1): W345-W349. https://doi.org/10.1093/nar/gkz424

Jensen, F., 2001. Polarization consistent basis sets: Principles. J. Chem. Phys., 115(20): 9113-9125. https://doi.org/10.1063/1.1413524

Keppler, D., 2014. The roles of MRP2, MRP3, OATP1B1, and OATP1B3 in conjugated hyperbilirubinemia. Drug Metab. Dispos., 42(4): 561-565. https://doi.org/10.1124/dmd.113.055772

Khusro,A.,Aarti,C.,Salem,A.Z.M.,Pliego,A.B.and Rivas-Caceres, R.R., 2020. Methyl-coenzyme M reductase (MCR) receptor as potential drug target for inhibiting methanogenesis in horses using *Moringa oleifera* L.: An *in silico* docking study. J. Equine Vet. Sci., 88(102949): 102949. https://doi.org/10.1016/j.jevs.2020.102949

Kim, S., Chen, J., Cheng, T., Gindulyte, A., He, J., He, S. and Bolton, E.E., 2023. PubChem 2023 update. Nucl. Acids Res., 51(D1): D1373-D1380. https://doi.org/10.1093/nar/gkac956

Koopmans, T., 1934. Über die Zuordnung von Wellenfunktionen und Eigenwerten zu den einzelnen Elektronen eines Atoms. Physica, 1(1-6): 104-113. https://doi.org/10.1016/S0031-8914(34)90011-2

Laskowski, R.A., MacArthur, M.W., Moss, D.S. and Thornton, J.M., 1993. Procheck: A program to check the stereochemical quality of protein structures. J. Appl. Crystallogr., 26(2): 283-291. https://doi.org/10.1107/S0021889892009944

Najmi, A., Javed, S.A., Al-Bratty, M. and Alhazmi, H.A., 2022. Modern approaches in the discovery and development of plant-based natural products and their analogues as potential therapeutic agents. Molecules, 27(2): 349. https://doi.org/10.3390/molecules27020349

Parr, R.G. and Pearson, R.G., 1983. Absolute hardness: Companion parameter to absolute electronegativity. J. Am. Chem. Soc., 105(26): 7512-7516. https://doi.org/10.1021/ja00364a005

Parsegian, V.A., 2005. Van der waals forces: A handbook for biologists, chemists, engineers, and physicists. Cambridge University Press. https://doi.org/10.1017/CBO9780511614606

Pitchers, K.G., Boakye, O.D., Campeotto, I. and Daly, J.M., 2024. The potential of plant-produced virus-like particle vaccines for African horse sickness and other equine orbiviruses. Pathogens, 13(6): 458. https://doi.org/10.3390/pathogens13060458

Raj, U. and Varadwaj, P.K., 2016. Flavonoids as multi-target inhibitors for proteins associated with Ebola virus: *In silico* discovery using virtual screening and molecular docking studies. Interdiscip. Sci., 8(2): 132-141. https://doi.org/10.1007/s12539-015-0109-8

Roy, P., 2013. Orbiviruses. In: Fields Virology 6th Ed. (Howley PM, Lippincott Williams DM, eds.) pp. 1402-1424.

Singh, D.B., 2020. Computer-aided Drug Design. Singapore: Springer. https://doi.org/10.1007/978-981-15-6815-2

Ukwubile, C.A., Malgwi, T.S., Angyu, A.E., Otalu, O. and Bingari, M.S., 2020. Review of antiviral medicinal plants used in Taraba State Nigeria: A possible source for COVID-19 drug discovery. J. Sci. Res. Med. Biol. Sci., 1(2): 1-23. https://doi.org/10.47631/jsrmbs.v1i2.50

Van Rijn, P.A., Maris-Veldhuis, M.A., Grobler, M., Wright, I.M., Erasmus, B.J., Maartens, L.H. and Potgieter, C.A., 2020. Safety and efficacy of inactivated African horse sickness (AHS) vaccine formulated with different adjuvants. Vaccine, 38(45): 7108-7117. https://doi.org/10.1016/j.vaccine.2020.08.072

Waterhouse, A., Bertoni, M., Bienert, S., Studer, G., Tauriello, G., Gumienny, R. and Schwede, T., 2018. Swiss-Model: Homology modelling of protein structures and complexes. Nucl. Acids Res., 46(W1): W296-W303. https://doi.org/10.1093/nar/gky427

Weyer, C.T., Grewar, J.D., Burger, P., Rossouw, E., Lourens, C., Joone, C. and Guthrie, A.J., 2016. African horse sickness caused by genome reassortment and reversion to virulence of live, attenuated vaccine viruses, South Africa, 2004–2014. Emerg. Infect. Dis., 22(12): 2087-2096. https://doi.org/10.3201/eid2212.160718

Wiederstein, M. and Sippl, M.J., 2007. ProSA-web: Interactive web service for the recognition of errors in three-dimensional structures of proteins. Nucl. Acids Res., 35: W407-W410. https://doi.org/10.1093/nar/gkm290